Prediction and Observation of Pocket Vibrational Modes in Crystals

K. W. Sandusky and J. B. Page
Department of Physics and Astronomy, Arizona State University, Tempe, Arizona 85287-1504

A. Rosenberg, C. E. Mungan, and A. J. Sievers
Laboratory of Atomic and Solid State Physics and Materials Science Center, Cornell University, Ithaca, New York 14853-2501
(Received 23 May 1991)

A perturbed-shell-model calculation for the impurity system KI:Ag^+ predicts three nearly-degenerate localized gap modes of different symmetry and unusual amplitude patterns: The displacements of the defect's fourth-nearest neighbors are more than an order of magnitude larger than those of the impurity or its nearest neighbors. Far-infrared isotope-effect measurements directly confirm the existence of these localized pocket modes.

PACS numbers: 78.30.−j, 63.20.Pw

Localized vibrational modes with maximum amplitude at or near the defect site have been investigated since the early 1960s [1–3]. In this paper, we show with the aid of the shell model a strikingly new type of localized mode in which the maximum vibrational amplitude occurs far removed from the defect site. We then present and analyze new isotope-effect experiments which directly confirm the existence of the unusual amplitude patterns associated with these localized "pocket" modes.

Previous experimental and theoretical studies [4–6] have shown that the substitutional silver ion in KI forms a nearly unstable defect-host combination at low temperatures: At $T=1.2$ K, the Ag^+ occupies the normal K^+ lattice site, but by 20 K it has moved to an as yet incompletely determined off-center configuration. The zero-temperature on-center dynamics are consistent with a perturbed harmonic shell model involving substantial force-constant softening [6]. Each Ag^+ impurity is characterized by its mass and by assumed defect–first-neighbor and relaxation-induced first-neighbor–fourth-neighbor longitudinal force-constant changes, obtained by fitting the observed ir-active T_{1u} resonance and gap mode frequencies at 17.3 and 86.2 cm^{-1}; all other force constants are assumed to be unperturbed. The model then predicts an E_g resonance at 20.5 cm^{-1}, in good agreement with the observed Raman peak at 16.1 cm^{-1}, and gap modes of A_{1g} and E_g symmetry with Raman strengths too weak to be observed [6].

The present study reveals that these three gap modes have some novel properties. First, despite their different symmetries, they are nearly degenerate: The predicted frequencies are 87.2, 86.0, and 86.2 cm^{-1} for the A_{1g}, E_g, and T_{1u} gap modes, respectively. Second, the computed displacement patterns for all three of these modes are strongly peaked on sites *away from* the Ag^+ defect and its nearest neighbors, namely, at the fourth-nearest-neighbor potassium ions [i.e., the $\pm(200)$, $\pm(020)$, and $\pm(002)$ ions]. Figures 1(a)–1(c) show the normalized displacements in these modes for ions along the $\pm(100)$ directions; the calculated displacements for all ions other than those along the six (100) directions are negligible. By contrast, Fig. 1(d) shows the computed displacement pattern for the 17.3-cm^{-1} T_{1u} resonant model, which is peaked at the impurity. Each of the computed gap modes thus consists of localized pockets of displacements on the six (100) axes, and we see from the figure that within each pocket the ions' relative motions are remarkably similar for all three symmetry types. The nearly-

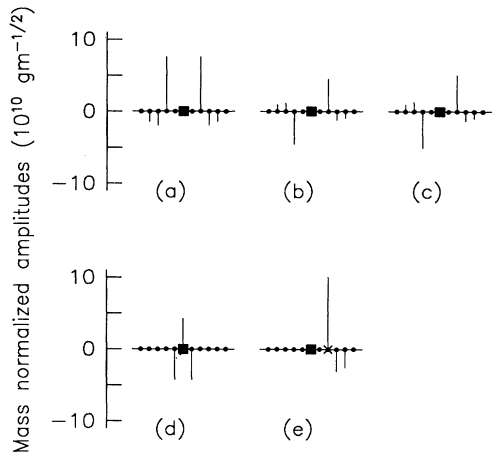

FIG. 1. Computed mass-normalized mode displacement patterns for KI:Ag^+. The defect is represented by a square. The displacements are plotted vertically, for ions along just the $\pm(100)$ directions, for ease of drawing; however, all displacements are actually longitudinal, i.e., directed along $\pm(100)$. (a) $T_{1u}(x)$, (b) A_{1g}, and (c) $E_g(2)$ pocket gap modes. [Note that (b) and (c) appear identical because only one axis is shown.] Here $T_{1u}(x)$ denotes the T_{1u} partner which couples to x-polarized infrared radiation, and $E_g(2)$ is the E_g partner which mixes with $T_{1u}(x)$ under a (200) $^{39}K \rightarrow {}^{41}K$ host-lattice isotopic substitution. For comparison, panels (d) and (e) show the patterns for the 17.3-cm^{-1} $T_{1u}(x)$ resonance and for the 84.7-cm^{-1} (200) isotopically shifted mode, respectively; in the latter, the symbol × denotes the $^{41}K^+$ isotope.

degenerate frequencies are apparently determined by the local dynamics within each of the pockets, which are weakly coupled to produce the different symmetry modes. Moreover, the fact that the defect's nearest neighbors have negligible displacements in the A_{1g} and E_g gap modes is consistent with these modes' weak Raman activity, since defect-induced first-order Raman scattering in alkali halides typically arises from the modulation of the electronic polarizability by the motion of the ions in the impurity's immediate vicinity. On the other hand, the T_{1u} gap mode, whose displacement pattern is similarly localized away from the defect, is readily observed with infrared radiation, since this probe couples to the mode's dipole moment regardless of where in the crystal it arises.

A direct verification of the existence of the A_{1g} and E_g gap modes is afforded by the occurrence in the host of two potassium isotopes: ^{41}K with 7% natural abundance, and ^{39}K with 93%. The presence of one or more of these $^{41}K^+$ ions on the fourth-nearest-neighbor sites results in strong mixing of the A_{1g}, E_g, and T_{1u} gap modes, producing three new ir-active gap modes.

To compute the mixing of the gap modes, we apply first-order nearly-degenerate perturbation theory to a single defect-isotope combination. The perturbed frequencies ω and zeroth-order displacement patterns are determined by the 6×6 eigenvalue problem

$$(\boldsymbol{\omega}_0^{-1}\mathbf{A}\boldsymbol{\omega}_0^{-1}-\omega^{-2}\mathbf{I})\mathbf{a}=0\,, \tag{1}$$

where the matrix $\mathbf{A}$ is given by

$$A_{ff'}=\delta_{ff'}+\boldsymbol{\chi}^{\dagger}(f)\Delta\mathbf{M}\boldsymbol{\chi}(f')\,.$$

Here $\boldsymbol{\chi}(f)$ is the unperturbed (no isotope) mass-normalized displacement eigenvector for the fth gap mode and $\Delta\mathbf{M}$ is the 3×3 isotope mass perturbation matrix. The matrix $\boldsymbol{\omega}_0$ is a diagonal matrix formed from the unperturbed gap mode frequencies. The components a_f of the eigenvector $\mathbf{a}$ determine the zeroth-order displacement patterns $\boldsymbol{\psi}$ as linear combinations of the unperturbed gap mode displacement eigenvectors: $\boldsymbol{\psi}=\sum_f a_f\omega_{0f}^{-1}\boldsymbol{\chi}(f)$. The sum runs over all six of the unperturbed gap modes: A_{1g} (nondegenerate), E_g (twofold degenerate), and T_{1u} (threefold degenerate).

Our computed splittings for the case of a single Ag^+ defect with a fourth-neighbor (200) $^{41}K^+$ substitution are shown in Fig. 2, which includes the shifted modes' percent relative absorption strengths for x-polarized radiation. The computed displacement pattern corresponding to the strongest shifted mode, at 84.7 cm^{-1}, is shown in Fig. 1(e); it consists mainly of E_g and T_{1u} components. We find that single isotopic substitutions on other K^+ sites produce shifts of less than 0.1 cm^{-1}, which are not individually resolvable.

To predict the experimentally observable absorption spectrum, calculations like those leading to Fig. 2 are carried out for the different defect-isotope configurations, and the results are combined with the configurations' probabilities [7]. Our calculated strengths for lines unresolvable from the 86.2-cm^{-1} line are included in that line's strength. The experimentally observable predictions [8] are given in the first column of Table I.

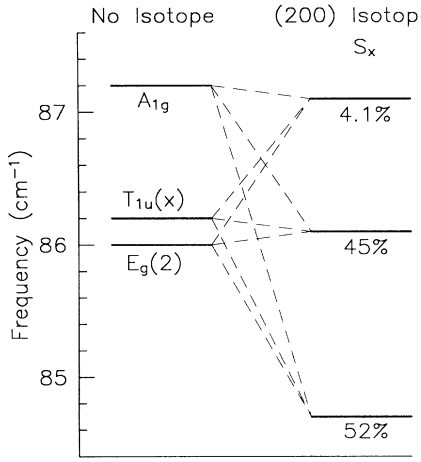

FIG. 2. Mixing of the three nearly-degenerate A_{1g}, $E_g(2)$, and $T_{1u}(x)$ gap modes under a (200) $^{39}K\rightarrow{}^{41}K$ host-lattice isotopic substitution. The percentages give the strengths S_x of the x-polarized absorption per defect/(200) isotope combination relative to a defect with no isotope substitution. Note that the percentages add up to slightly more than 100% because the absorption coefficient is not only proportional to the imaginary part of the dielectric function but also inversely proportional to the host-crystal index of refraction, which is strongly frequency dependent in the gap mode region.

Figure 3 shows the far-ir absorption spectra at several temperatures for a sample of KI+0.1 mol% AgI. The strong features in this spectral region are the unperturbed $^{39}KI:Ag^+$ gap mode [9] at 86.2 cm^{-1} and the $^{35,37}Cl^-$ doublet at 77.1 and 76.8 cm^{-1}. Note that, in contrast to the temperature independence of the Cl^- modes, the Ag^+ gap mode exhibits a marked temperature dependence: Its strength vanishes by 25 K [4,6]. Of interest here is the weak line at 84.5 cm^{-1}, identified by the arrow. The large shift and small strength of this line preclude the possibility of its being a Ag^+ isotope mode. However, as shown in Fig. 4, the 84.5-cm^{-1} line has a temperature dependence similar to that of the unper-

TABLE I. Calculated and measured gap mode splittings and strengths for KI:Ag^+ due to 7% isotopic abundance of $^{41}K^+$ in the host crystal, relative to the unperturbed gap mode at 86.2 cm^{-1}. Only one observable isotopic line is predicted and observed.

	Calculated	Measured
Frequency (cm^{-1})	84.7	84.5
Frequency splitting (cm^{-1})	−1.5	−1.7
Relative strength	0.07	0.04

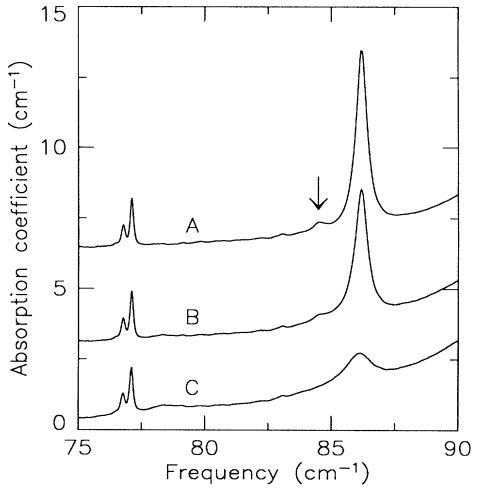

FIG. 3. Absorption spectra of KI+0.1% AgI over part of the phonon gap region of KI. The resolution is 0.1 cm^{-1}. The strong line at 86.2 cm^{-1} is the unperturbed Ag^+ gap mode. The doublet at 77.1 and 76.8 cm^{-1} is due to $^{35,37}Cl^-$ impurity isotopes. The arrow at 84.5 cm^{-1} points out the newly observed mode produced by $^{41}K^+$ substitution on the fourth neighbor of the Ag^+ defect. The temperatures of the spectra are *A*, 1.4 K; *B*, 7.6 K; and *C*, 13.7 K.

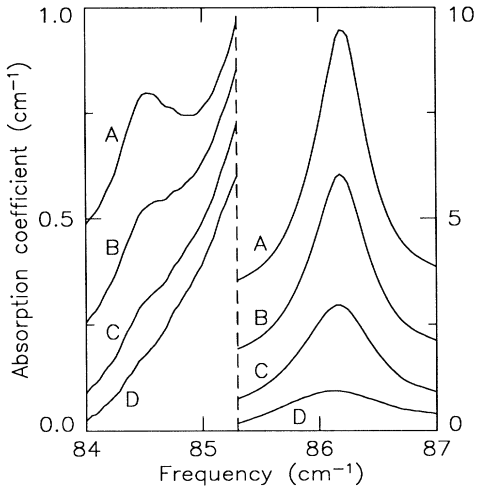

FIG. 4. Absorption coefficient of KI+0.1% AgI. The results are from Fig. 3 but on an expanded scale. Note the different vertical scales in the two halves. The temperature dependence of the weak line at 84.5 cm^{-1} is similar to that of the much stronger unperturbed Ag^+ gap mode. The temperatures of the spectra are *A*, 1.4 K; *B*, 7.6 K; *C*, 10.0 K; and *D*, 13.7 K.

turbed Ag^+ gap mode. Both the strong and the weak lines are characterized by center frequencies and linewidths which change only slightly, and by strengths which disappear, over this temperature range. On the basis of this shared temperature behavior, which is a signature of Ag^+ in KI, we attribute this newly observed weak line to the Ag^+ center.

In order to quantify the temperature dependence of this 84.5-cm^{-1} mode, we determined the strengths of the two Ag^+ lines at each temperature. First, we found the shape of the temperature-dependent difference-band phonon absorption by fitting the data from 40 to 92 cm^{-1}, with all absorption lines deleted, to a polynomial which was subtracted from the data. Finally, we fitted the Ag^+ lines by the sum of two Voigt functions [10] of the same width, using the amplitudes of the two lines and the position and width of the strong line as fitting parameters. In this last step, we determined this splitting (assumed temperature independent) from the lowest-temperature data, where the two lines were clearly resolved (see Figs. 3 and 4). The resulting temperature-dependent strength of the weak line is shown in Fig. 5. The dashed curve gives the temperature dependence of the strong line as determined by this and earlier work [6]. Within experimental error, the temperature dependences of the strengths of the two lines are the same.

In terms of our model, we identify the weak 84.5-cm^{-1} line in the spectrum with the lowest-frequency ir-active mode produced by $^{41}K^+$ substitution on the fourth neighbor of the Ag^+ defect, as shown in Fig. 2; its computed displacement pattern is shown in Fig. 1(e). Of the three modes shown in Fig. 2, only the lowest-frequency one is predicted to have both a large enough splitting (1.5 cm^{-1}) and sufficient strength (7.0%) relative to the unperturbed KI:Ag^+ gap mode to be resolvable, and indeed it is the only isotope line we have observed. As summarized in Table I, the experimental findings of a shift of 1.7 cm^{-1} and a relative strength of 4% are in good agreement with the predictions of the model, especially since the calculations involve no free parameters and neglect anharmonic corrections. The predicted 86.1-cm^{-1} isotope mode has a shift of only 0.1 cm^{-1}, much smaller

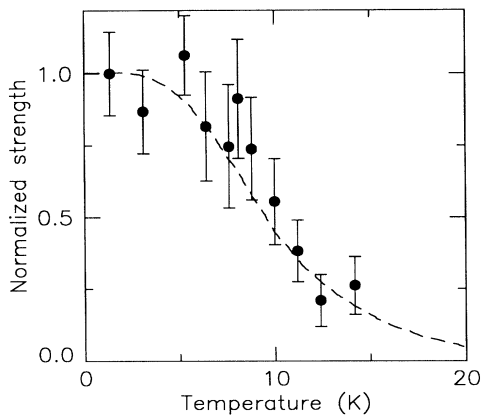

FIG. 5. Temperature dependence of the strengths of the two ir-active modes produced by the Ag^+ center in the KI gap region. The solid circles are the data for the weak mode at 84.5 cm^{-1}, produced by $^{41}K^+$ substitution on the fourth neighbor of the Ag^+ defect; the dashed line gives the temperature dependence of the unperturbed Ag^+ gap mode at 86.2 cm^{-1}.

than the experimental low-temperature linewidth (0.5 cm^{-1}) of the strong 86.2-cm^{-1} line, while the predicted 87.1-cm^{-1} isotope mode has a relative strength of only 0.6%.

In our model, the large force-constant weakening derives from the presence of the low-frequency 17.3-cm^{-1} T_{1u} resonance and the 86.2-cm^{-1} T_{1u} gap mode in the KI:Ag^+ system at $T=0$ K, raising the question as to whether or not pocket gap modes might be a general feature of impurity systems which have low-frequency resonances and large host-crystal phonon gaps. To test this idea, we can consider the system NaI:Cl^-, which has an even lower-frequency infrared resonance, at 5.4 cm^{-1}, and a wide unperturbed phonon frequency gap [11,12]. Accordingly, we have applied the present model to this system and found that for all force-constant changes consistent with the 5.4-cm^{-1} resonance, the predicted gap modes are in fact localized at the defect site, in striking contrast to the pocket mode behavior established here for KI:Ag^+. This suggests that an additional key feature may be the location relative to the defect of the heavy and light host-lattice constituents, which necessarily have disparate masses in order to produce large phonon gaps—in KI:Ag^+ and NaI:Cl^- the light constituents are the defect's fourth-nearest neighbors (200) and first-nearest neighbors (100), respectively. We have therefore carried out preliminary model calculations for the hypothetical "inverse" systems NaI:Ag^+ and KI:Cl^-, with the force-constant changes obtained by assuming the existence of a T_{1u} resonant mode near zero frequency and a T_{1u} localized mode in the gap. We find pocket gap modes for the former case, but not for the latter; hence, these new localized modes are a general feature of a class of defect-lattice systems.

The work by K.W.S. and J.B.P. is supported by NSF Grant No. NSF-DMR-90-14729, and that by A.R., C.E.M., and A.J.S. is supported by NSF Grant No. NSF-DMR-89-18894 and ARO Grant No. ARO-DAAL03-90-G-0040.

[1] A. A. Maradudin, E. W. Montroll, G. H. Weiss, and I. P. Ipatova, *Theory of Lattice Dynamics in the Harmonic Approximation,* Solid State Physics Suppl. 3 (Academic, New York, 1971), 2nd ed.

[2] A. S. Barker, Jr., and A. J. Sievers, Rev. Mod. Phys. **47**, Suppl. 2, S1 (1975).

[3] H. Bilz, D. Strauch, and R. K. Wehner, *Handbuch der Physik* (Springer-Verlag, Berlin, 1984), Vol. XXV, Pt. 2d.

[4] A. J. Sievers and L. H. Greene, Phys. Rev. Lett. **52**, 1234 (1984).

[5] S. B. Hearon and A. J. Sievers, Phys. Rev. B **30**, 4853 (1984).

[6] J. B. Page, J. T. McWhirter, A. J. Sievers, H. Fleurent, A. Bouwen, and D. Schoemaker, Phys. Rev. Lett. **63**, 1837 (1989).

[7] D. Bäuerle, *Vibrational Spectra of Electron and Hydrogen Centers in Ionic Crystals,* Springer Tracts in Modern Physics Vol. 68 (Springer-Verlag, Berlin, 1973), p. 130.

[8] In obtaining these results, we have included the (small) contributions of Ag^+ impurities having a pair of opposite fourth-neighbor [(200) and −(200)] $^{41}K^+$ isotopes.

[9] We have found that the Ag^+ T_{1u} gap mode frequency is concentration dependent. For zero concentration the extrapolated frequency is 86.1 cm^{-1}.

[10] B. Di Bartolo, *Optical Interactions in Solids* (Wiley, New York, 1968), p. 366.

[11] B. P. Clayman, I. G. Nolt, and A. J. Sievers, Solid State Commun. **7**, 7 (1969).

[12] J. B. Page and K. G. Helliwell, Phys. Rev. B **12**, 718 (1975).